



## THE MAPPING OF TEA HARVESTING AREA USING PLANETSCOPE IMAGERY

Wikan Jaya Prihantarto<sup>12</sup>, Eva Purnamasari<sup>1</sup>, Muhammad Ismail<sup>1</sup>, Kurnia Anggraini<sup>1</sup>, Mufid Amafi<sup>1</sup>, Natratal Zahira<sup>1</sup>, Citra Sri Ramadhani<sup>1</sup>, Andre<sup>1</sup>, Hendry Frananda<sup>3</sup>, Erisa Ayu Waspadia Putri<sup>24</sup>, Indah Setiawati<sup>25</sup>

<sup>1</sup>Remote Sensing and Geographic Information System, Vocational School, Universitas Negeri Padang, Padang 25131, Indonesia

<sup>2</sup>Natural Resources and Environmental Management, Graduate School, IPB University, 16680, Bogor, West Java, Indonesia

<sup>3</sup>Geography Department, Universitas Negeri Padang, 25171 Padang, Indonesia

<sup>4</sup>Forestry Department, Faculty of Forestry, Universitas Tanjungpura, Pontianak 78116, Indonesia

<sup>5</sup>Agribusiness Study Program, Faculty of Agriculture, Department of Agricultural Social and Economy, Universitas Jenderal Soedirman, 53123, Purwokerto, Central Java, Indonesia

Email : wikanjaya@fis.unp.ac.id

**ABSTRACT:** *The identification of tea harvesting areas is an important part of tea culture. The use of satellite imagery for this application offers effectiveness. PlanetScope imagery has the advantage of high spatial, spectral, and temporal resolution and is widely used in agricultural and plantation studies. The objective of this study was to map tea pruning areas in the Danau Kembar Tea Plantation, Solok Regency, West Sumatra, using PlanetScope imagery. The images underwent radiometric, geometric correction and were then analyzed spectrally using the Normalized Difference Vegetation Index (NDVI) to obtain tea vegetation density classes. The image map resulting from this classification was used to identify the spatial distribution of harvesting and non-harvesting areas. The mapping results were validated by field surveys, and accuracy calculations were performed using the confusion matrix method. The findings showed that 250.50 hectares or 90.37% of the study area, are harvesting areas, with mapping accuracy reaching 84.0%. This study can provide an important reference for monitoring plantation land management, production estimation, and tea harvesting.*

*Keywords:* tea plantation, harvesting area, planetscope, mapping

### 1. INTRODUCTION

Indonesia has long been recognized as one of the world's largest tea (*Camelia sinensis*) producers, a reputation that makes the country a strategic supplier in the global supply chain. More than just an export commodity that contributes to the country's foreign exchange, the tea industry plays a vital role in the people's economic structure, particularly as an employer in rural areas (Manumono & Listiyani, 2023). West Sumatra, for example, is known as one of the strategic tea production centers in Indonesia. In this region, PTPN IV Danau Kembar stands as a leading agribusiness entity specializing in black tea production. Despite its massive production potential, this plantation faces a classic but crucial challenge, inefficiency in plantation monitoring (Dengia et al., 2023; Lavenia & Rinanda Saputri, 2023). This problem is not unique to PTPN IV, but rather a reflection of the challenges faced by the national tea plantation industry in general. Amid the threat of global climate change, which is making weather patterns increasingly unpredictable, data accuracy is key to agribusiness sustainability (Fatawa et al., 2023). Therefore, the need for innovative monitoring tools to support sustainable plantation practices is becoming increasingly urgent.

In tea plantation management, harvesting is not just a routine activity, but rather a core operational task that requires precise management. Therefore, monitoring of areas ready for harvest is a crucial aspect. This monitoring process plays a vital role as it is the main determinant of the sustainability of the plantation business cycle. Accurate monitoring data is needed to synchronize harvesting rotations, schedule plant maintenance, and compile valid production estimates. To support this managerial complexity, remote sensing technology is now widely adopted as a strategic solution. This technology offers the advantage of a synoptic overview, which is the ability to provide a comprehensive and simultaneous view of a large area. These benefits can support plantation management, such as the identification of spatial conditions of plants efficiently and effectively compared to conventional survey

methods (Khanal et al., 2020; Omia et al., 2023; Weiss et al., 2020). Conventional methods in identifying harvest areas generally rely on historical production records or manual field monitoring surveys. This method often has limitations in that it is less reliable in capturing spatial variability in the field and less accurate in terms of time. As an alternative technology-based solution, remote sensing offers scalability for agricultural monitoring (Waspadi & Danoedoro, 2019).

In the cultivation of perennial crops such as tea, where canopy conditions can vary greatly between blocks due to pruning or pest attacks, high-resolution satellite imagery is an unavoidable necessity. PlanetScope is one of the leading technological breakthroughs with dense temporal coverage (almost daily) and fine spatial detail (Rafif et al., 2021). The technical advantages of PlanetScope are significant, as explained by (Skakun et al., 2021), its 8-band sensor and 3-meter spatial resolution can increase the accuracy of crop production estimates by up to 77% compared to other popular resource satellites, such as Sentinel and LANDSAT variants. This sharper resolution enables the detection of phenological changes, crop responses to agronomic treatments, and the identification of specific management zones within a single field (Kaya et al., 2025; Liu et al., 2025; Parida et al., 2024).

Scientifically, the identification of plantation crop characteristics using remote sensing data can be done through an empirical approach that links in situ (field) data with spectral indices, particularly the Vegetation Index (VI). (Yan et al., 2025) summarizes that VI is highly sensitive to the biophysical, biochemical, and physiological characteristics of plants. Among various indices, the Normalized Difference Vegetation Index (NDVI) is the most widely applied in this field (Nițu et al., 2025). NDVI serves as a variable that describes photosynthetic activity, enabling quantitative correlations between vegetation conditions such as vegetation health and crop productivity. Previous studies in tea plantations have confirmed a strong relationship between NDVI and tea bud production. Siahaan et al. (2024) reported a coefficient of determination exceeding 57.6%. Furthermore, cross-country research by Phan et al. (2020) in Vietnam, Ramzan et al. (2023) in Pakistan, and dan Rama Rao et al. (2007) in India showed significant results with an accuracy above 70% and coefficient determination value above 0.80.

Based on this background, this study aims to identify effective harvesting areas for tea plantations at PTPN IV, Danau Kembar Unit, Solok Regency, West Sumatra, using PlanetScope satellite imagery. In addition, this study also aims to test validity by comparing the accuracy of interpretations with field observation data.

## 2. METHODS

### 2.1 Research Location

This study was conducted at Tea Plantation estate of Afdeling B, PTPN IV Danau Kembar. located in Solok Regency, West Sumatra, Indonesia, the extent of this estate is about 284.76 hectares that stretches between 100°37'8.893"E, 0°58'33.75"S and 100°38'51.994"E, 1°0'21.65"S. This estate consist of 28 blocks. The area is situated at an elevation of approximately 1,300–1,600 meters above sea level with a tropical highland climate zone, characterized by annual rainfall of 2,500–3,000 mm and an average temperature of 18–25°C. the detail of study area showed in .

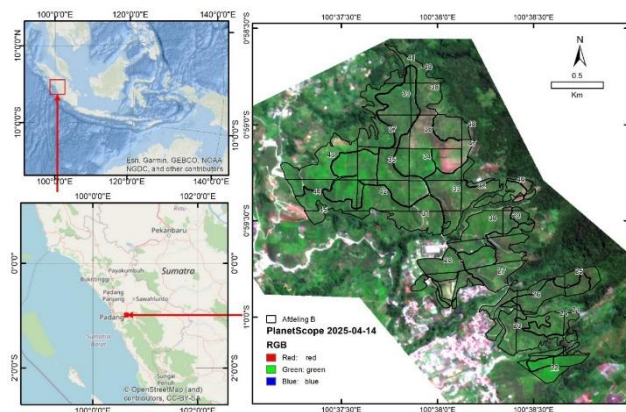


Figure 1 Research Area



### 2.2. Data and Material

PlanetScope satellite imagery was used as primary data source for this study, obtained on April 14<sup>th</sup>, 2025. The images had a spatial resolution of 3 meters and consist of 8 bands. Detail of image specification used can be seen in Table 1. The secondary data used are block maps in Afdeling B obtained from PTPN IV Danau Kembar. The 1:25,000 scale Indonesian Topographic (RBI) Map published by the Indonesian Geospatial Information Agency (BIG) was used as additional material for geographical reference and guidance in conducting field validation.

Variable	Detail
Sensor	PSD.SD
Product Type	Analytic Surface Reflectance
Image Acquisition	April 14 <sup>th</sup> 2025
Spatial Resolution	3 m
Radiometric Resolution	16 bit
Cloud Cover	0%
Off nadir	3.1°
Format Data	TIFF
Spectral Resolution	<ol style="list-style-type: none"> <li>1. Coastal Blue: 431 – 452 nm</li> <li>2. Blue: 465 – 515 nm</li> <li>3. Green I (Green): 515 – 550 nm</li> <li>4. Green: 547 – 584 nm</li> <li>5. Yellow: 600 – 620 nm</li> <li>6. Red: 630 – 685 nm</li> <li>7. Red Edge: 695 – 730 nm</li> <li>8. Near-Infrared (NIR): 758 – 885 nm</li> </ol>

Table 1 Image specification

### 2.3. Research Method

#### 2.2.1. Image Pre-processing

Citra PlanetScope underwent preprocessing in the form of geometric correction based on RBI map using image-to-map method. This process is carried out to ensure positional accuracy based on legitimate geographical references. Next, radiometric calibration is performed by converting the original pixel values to surface reflectance (REF). Formula (1) is used in this process.

$$REF(i) = RAD(i) \frac{\pi * SD^2}{EAI(i) * \cos(SZ)} \quad (1)$$

The radiance value (RAD) on each band (i) is used as input. This formula also involves the solar zenith angle (SZ) and the distance between the Earth and the Sun at the time of acquisition (SD), both of which can be found in the image metadata (Huang & Roy, 2021). The Exo-Atmospheric Irradiance (EAI) value is a standard value used in the image calibration process. Planet simplifies the calibration process with the conversion formula as presented in (2).

$$REF(I) = DN(i) * RC(i) \quad (2)$$

The formula simply converts the original value of the digital number (DN) by multiplying it by the Reflectance Coefficient (RC) (Frazier & Hemingway, 2021). These values are available in each PlanetScope product metadata and vary based on the conditions when the data was acquired by the satellite. The images that have been corrected geometrically and radiometrically are then cropped according to the vector block map data of Afdeling B. This process is important to filter the study area and ensure that no land cover outside the plantation area is included in the process.



### 2.2.2. Image Interpretation

To identify and map harvesting areas, image interpretation used a hybrid method that combines digital and visual techniques. The initial stage of digital interpretation was carried out using NDVI transformation. This method involves red ( $i_8$ ) and infrared ( $i_6$ ) images and is calculated using formula (3). NDVI was chosen because of its ability to represent plant vegetative development and biomass estimation (Anurogo et al., 2018; Purnamasari et al., 2024). The spectral index has also proven to be robust in its application for estimating agro-industrial crop production and effective across a range of agroclimatic characteristics.

$$NDVI = \frac{(i_8 - i_6)}{(i_8 + i_6)} \quad (3)$$

NDVI values are reclassified according to the estimated vegetation density level. At this stage, visual interpretation is used to divide the value range based on the appearance in the image. The elements of interpretation used in this process include color, texture, pattern, shadow, and association (Seidlova et al., 2021). Vegetation density classes are divided into five categories, i.e. very low, low, medium, high, and very high. The assumption is that the denser the tea vegetation, the closer it is to being ready for harvest.

### 2.2.3. Accuracy Assessment

To ensure the reliability of the detection model, a rigorous validation process was executed by comparing the predicted class of harvesting area against the actual validation data derived from field survey. Field survey were conducted by selecting a number of samples purposively based on a tentative vegetation density map. The information collected in the field was the actual conditions, accompanied by coordinate recordings using handheld GPS devices.

The classification scheme adopted a binary nominal scale, categorizing features into two distinct classes: harvesting area and non-harvesting area. The accuracy assessment was quantified using a confusion matrix, a standard framework for evaluating classification performance. This matrix facilitates a cross-tabulation between the predicted values and the reference objects, segmenting the results into four fundamental partitions i.e. True Positive (TP), True Negative (TN), False Positive (FP), and False Negative (FN) (Chicco & Jurman, 2020; Chugh et al., 2020). The cross-tabulation of the four cases can be seen in Table 2.

Actual	Prediction	
	Harvesting Area	Non-Harvesting Area
Harvesting Area	true positive (TP)	false negative (FN)
Non-Harvesting Area	false positive (FP)	true negative (TN)

Table 2 Confusion matrix of harvesting area identification

The assessment of the model's performance was conducted using a suite of statistical metrics: Precision, Recall, and F1 Score. Total Accuracy serves as a measure of overall effectiveness, estimated by calculating the ratio of correctly classified instances to the total population tested, as denoted in Equation (1). Precision quantifies the reliability of positive predictions; it is defined as the ratio of correct positive predictions (TP) to the total number of instances predicted as positive, as presented in Equation (2). Recall, synonymous with sensitivity, measures the model's ability to identify all relevant instances, represented by the True Positive Rate in Equation (3). Finally, the F1 Score (Equation 4) is utilized as a balanced metric; it is calculated as the harmonic mean of precision and recall, providing a single score that accounts for both false positives and false negatives (Chicco & Jurman, 2020). The following is the formula used to calculate the three metrics' values.

$$Accuracy = \frac{TP+TN}{TP+TN+FP+FN} \quad (1)$$

$$Precision = \frac{TP}{TP+FP} \quad (2)$$



$$Recall = \frac{TP}{TP+FN} \quad (3)$$

$$F1\ score = 2 * \frac{Precision*Recall}{Precision+Recall} \quad (4)$$

### 3. RESULT AND DISCUSSION

Spectral analysis of the processed PlanetScope imagery revealed a broad range of NDVI values, spanning from 0.124 to 0.787, illustrating significant spatial heterogeneity in vegetation density across the estate. A critical threshold was established at an NDVI value of 0.511; areas falling below this benchmark were categorized as non-vegetated or pruning area. Consequently, tea vegetation (canopy) density was stratified into five distinct classes: very high, high, moderate, low, and very low (non-vegetated). The resulting spatial distribution of vegetation density is visualized in Figure 2.

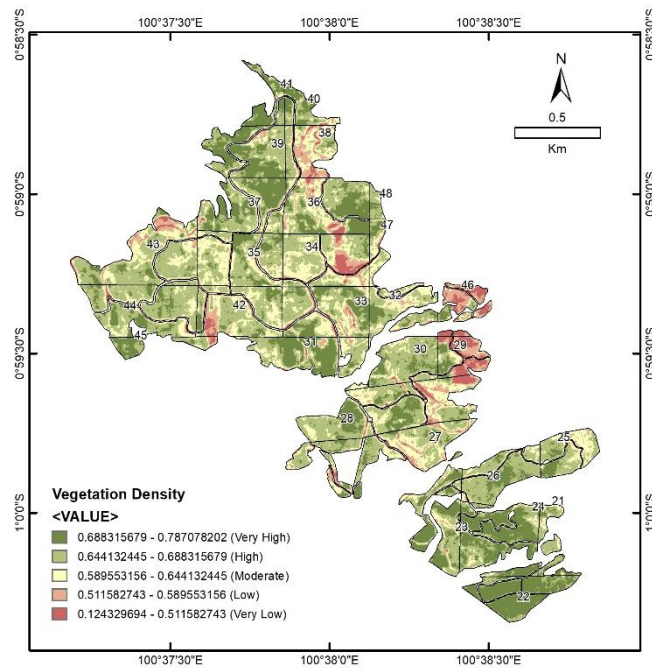


Figure 2 Vegetation density of tea plantation entire Afdeling B

From an agronomic perspective, the high and very high density classes correspond to tea bushes exhibiting dense foliage and abundant shoot proliferation, signaling optimal harvest readiness. In contrast, moderate and low density area reflect reduced canopy cover, typically indicative of recent plucking cycles or early stages of regrowth. The very low class primarily delineates pruning zones or non-vegetated infrastructure within the estate. Therefore, areas with low to very low vegetation density were classified as non-harvesting areas, while areas with moderate to very high vegetation cover were categorized as harvesting areas. The Figure 3 below shows the classification of vegetation density into harvesting areas in each block of Afdeling B.

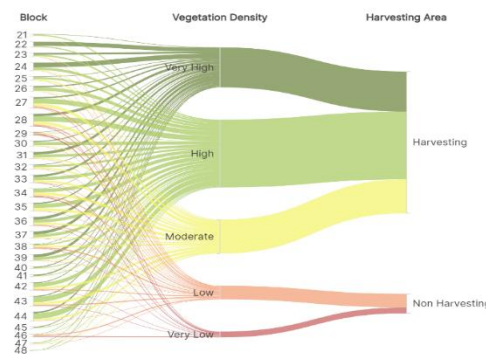


Figure 3 Classification of vegetation density to harvesting area in each block



The total area of the plantation studied was 284.76 hectares, with 250.50 hectares classified as harvesting ready area. On the other hand, 34.26 hectares of the area are classified as non-harvesting areas. The tentative harvesting area map produced was validated by field observations at predetermined sampling points. The spatial distribution of harvesting and non-harvesting areas is presented in Figure 4 below.

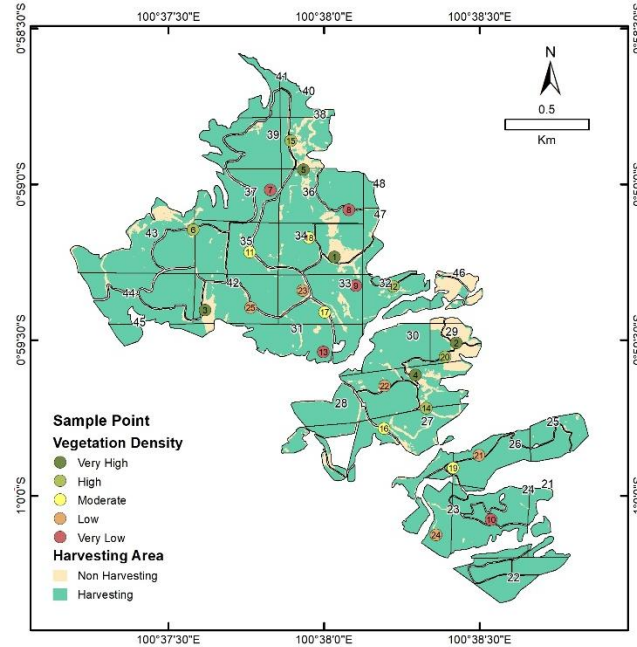


Figure 4 Spatial distribution of harvesting area and field survey sample point

The areas with high tea canopy density dominate, covering 119.81 hectares, followed by very high density areas covering 70.81 hectares and moderate areas covering 59.88 hectares. The area not included in the non-harvesting class is divided into 23.99 hectares with low vegetation cover and 10.27 hectares with very low vegetation cover. Details of the area of each harvesting class can be seen in Table 3.

Vegetation Density	Harvesting Area		Hectares
	Non-Harvesting	Harvesting	
Very High		70.81	70.81
High		119.81	119.81
Moderate		59.88	59.88
Low	23.99		23.99
Very Low	10.27		10.27
Total	34.26	250.50	284.76

Table 3 Recapitulation of harvesting area extent

Spatial quantification of Afdeling B revealed a total extent of 284.76 hectares, within which 250.50 hectares were delineated as harvesting area. This distribution implies a high land utility rate, with approximately 87.96 % of the total area dedicated to active tea production (harvesting area), leaving a residual 12.04% comprising maintenance area or non-harvesting area. Detailed analysis at the block level identified notable spatial discrepancies. Block 46 exhibited the most pronounced variance between total block size and active productive area, with a difference of 3.37 hectares; this suggests that a substantial portion of the block was on maintenance or remained underutilized during the observation period. In sharp contrast, Block 22, 41, and 48 demonstrated the highest land efficiency with minimal discrepancies, indicating near-total canopy coverage and optimal harvest readiness. These comparative findings underscore the spatial heterogeneity inherent in the estate's management practices and canopy distribution. Comparison of block and harvest area extent can be seen in Figure 5.

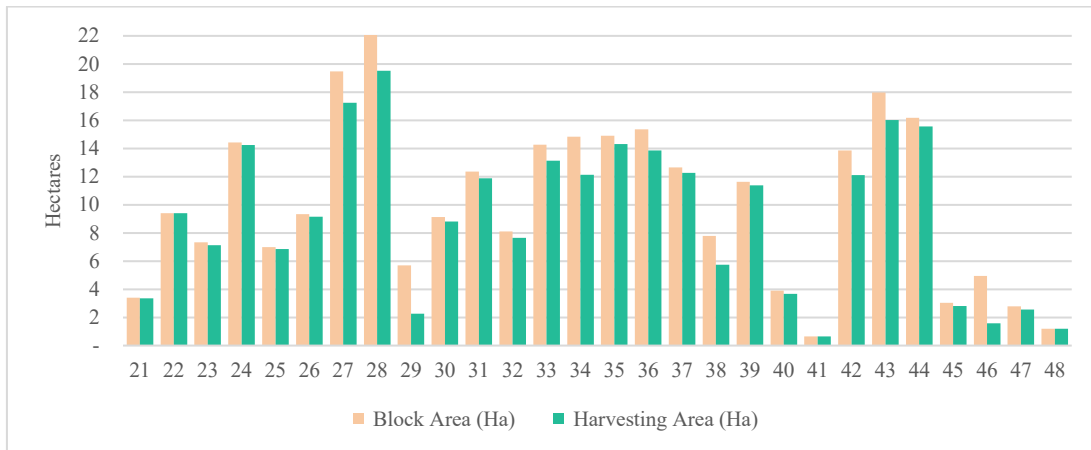


Figure 5 Comparison of block and harvest area

Based on field observations using harvest area maps of 25 samples, 12 locations from the harvest area class and 9 non-harvest area samples corresponded to actual conditions as shown in Table 4. The result demonstrated robust performance with an overall accuracy of 84.0% and an F1 Score of 85.7%, indicating a reliable balance between precision and sensitivity. High precision rate of 92.3% depict a strong capability to minimize commission errors. Although the recall value of 80.0% indicates a slight tendency towards omission errors, the overall metrics suggest that the map produced is stable for operational monitoring. Detail of accuracy metric value can be seen in Table 5.

Actual	Map		Total
	Harvesting Area	Non-Harvesting Area	
Harvesting Area	12	3	15
Non-Harvesting Area	1	9	10
Total	13	12	25

Table 4 Confusion matrix of harvesting area identification

Metric	Value
accuracy	84.0%
precision	92.3%
recall	80.0%
F1	85.7%

Table 5 Metric of accuracy assessment

The accuracy aligns with the typical acceptable threshold for vegetation classification, which generally ranges between 75% and 85% for heterogeneous canopy covers. This performance validates the high-resolution PlanetScope imagery in resolving the spectral complexities of tea plantations and distinguishing its spatial vegetation characteristics. Furthermore, the strong F1 score confirms that the chosen vegetation indices and classification thresholds were effective in distinguishing harvesting areas from other.

#### 4. CONCLUSION

The analysis shows that 250.50 hectares or 87.97% of the tea plantation area of Afdeling B, PTPN IV Danau Kembar is harvesting area, while the remaining 34.26 hectares (12.04%) is non-harvesting area. The mapping of the harvest area using PlanetScope imagery resulted in a total accuracy of 84%, which proved the reliability of the imagery in mapping the harvest area.



### REFERENCES

- [1] Anurogo, W., Sari, L. R., Lubis, M. Z., Pamungkas, D. S., Mufida, M. K., & Lestari Situmorang, A. D. (2018). An Integrated Comparative Approach to Estimating Forest Aboveground Carbon Stock Using Advanced Remote Sensing Technologies. *2018 International Conference on Applied Engineering (ICAE)*, 1–6. <https://doi.org/10.1109/INCAE.2018.8579375>
- [2] Chicco, D., & Jurman, G. (2020). The advantages of the Matthews correlation coefficient (MCC) over F1 score and accuracy in binary classification evaluation. *BMC Genomics*, *21*(1), 6. <https://doi.org/10.1186/s12864-019-6413-7>
- [3] Chugh, R. S., Bhatia, Vardaan, Khanna, K., & Bhatia, Vandana. (2020). A Comparative Analysis of Classifiers for Image Classification. *2020 10th International Conference on Cloud Computing, Data Science & Engineering (Confluence)*, 248–253. <https://doi.org/10.1109/Confluence47617.2020.9058042>
- [4] Dengia, A., Dechassa, N., Wogi, L., & Amsalu, B. (2023). A simplified approach to satellite-based monitoring system of sugarcane plantation to manage yield decline at Wonji-Shoa Sugar Estate, central Ethiopia. *Heliyon*, *9*(8), e18982. <https://doi.org/10.1016/j.heliyon.2023.e18982>
- [5] Fatawa, M. I., Santosa, E., Hapsari, D. P., & Krisantini. (2023). Climate change and its adaptation strategies on tea plantation in West Java, Indonesia. *Indonesian Journal of Agronomy*, *51*(2), 257–268. <https://doi.org/10.24831/ija.v51i2.47081>
- [6] Frazier, A. E., & Hemingway, B. L. (2021). A Technical Review of Planet Smallsat Data: Practical Considerations for Processing and Using PlanetScope Imagery. *Remote Sensing*, *13*(19), 3930. <https://doi.org/10.3390/rs13193930>
- [7] Huang, H., & Roy, D. P. (2021). Characterization of Planetscope-0 Planetscope-1 surface reflectance and normalized difference vegetation index continuity. *Science of Remote Sensing*, *3*, 100014. <https://doi.org/10.1016/j.srs.2021.100014>
- [8] Kaya, F., Ferhatoglu, C., & Başayığit, L. (2025). Multi-Temporal Normalized Difference Vegetation Index Based on High Spatial Resolution Satellite Images Reveals Insight-Driven Edaphic Management Zones. *AgriEngineering*, *7*(4), 92. <https://doi.org/10.3390/agriengineering7040092>
- [9] Khanal, S., KC, K., Fulton, J. P., Shearer, S., & Ozkan, E. (2020). Remote Sensing in Agriculture—Accomplishments, Limitations, and Opportunities. *Remote Sensing*, *12*(22), 3783. <https://doi.org/10.3390/rs12223783>
- [10] Lavenia, T., & Rinanda Saputri, F. (2023). Blynk App-Based Plant Monitoring System Design. *International Journal of Science and Environment (IJSE)*, *3*(4), 145–150. <https://doi.org/10.51601/ijse.v3i4.82>
- [11] Liu, H., Liu, Y., Xu, W., Wu, M., Wang, L., Lu, N., & Ou, G. (2025). A Seasonal Fresh Tea Yield Estimation Method with Machine Learning Algorithms at Field Scale Integrating UAV RGB and Sentinel-2 Imagery. *Plants*, *14*(3), 373. <https://doi.org/10.3390/plants14030373>
- [12] Manumono, D., & Listiyani. (2023). Kajian Perkembangan Teh di Indonesia. *AGRIFITIA: Journal of Agribusiness Plantation*, *2*(2), 133–146. <https://doi.org/10.55180/aft.v2i2.281>
- [13] Nițu, A., Florea, C., Ivanovici, M., & Racoviteanu, A. (2025). NDVI and Beyond: Vegetation Indices as Features for Crop Recognition and Segmentation in Hyperspectral Data. *Sensors*, *25*(12), 3817. <https://doi.org/10.3390/s25123817>
- [14] Omia, E., Bae, H., Park, E., Kim, M. S., Baek, I., Kabenge, I., & Cho, B.-K. (2023). Remote Sensing in Field Crop Monitoring: A Comprehensive Review of Sensor Systems, Data Analyses and Recent Advances. *Remote Sensing*, *15*(2), 354. <https://doi.org/10.3390/rs15020354>
- [15] Parida, B. R., Mahato, T., & Ghosh, S. (2024). Monitoring tea plantations during 1990–2022 using multi-temporal satellite data in Assam (India). *Tropical Ecology*, *65*(3), 387–398. <https://doi.org/10.1007/s42965-023-00304-x>
- [16] Phan, P., Chen, N., Xu, L., & Chen, Z. (2020). Using Multi-Temporal MODIS NDVI Data to Monitor Tea Status and Forecast Yield: A Case Study at Tanuyen, Laichau, Vietnam. *Remote Sensing*, *12*(11), 1814. <https://doi.org/10.3390/rs12111814>
- [17] Purnamasari, E., Kamal, M., Wicaksono, P., Hidayatullah, M. F., & Susetyo, B. B. (2024). Multi-spatial Resolution Imagery to Estimate Above-Ground Carbon Stocks in Mangrove Forests. *JOIV: International Journal on Informatics Visualization*, *8*(3), 1118. <https://doi.org/10.62527/joiv.8.3.2237>
- [18] Rafif, R., Kusuma, S. S., Saringatin, S., Nanda, G. I., Wicaksono, P., & Arjasakusuma, S. (2021). Crop Intensity Mapping Using Dynamic Time Warping and Machine Learning from Multi-Temporal PlanetScope Data. *Land*, *10*(12), 1384. <https://doi.org/10.3390/land10121384>
- [19] Rama Rao, N., Kapoor, M., Sharma, N., & Venkateswarlu, K. (2007). Yield prediction and waterlogging assessment for tea plantation land using satellite image-based techniques. *International Journal of*



- Remote Sensing*, 28(7), 1561–1576. <https://doi.org/10.1080/01431160600904980>
- [20] Ramzan, Z., Asif, H. M. S., Yousuf, I., & Shahbaz, M. (2023). A Multimodal Data Fusion and Deep Neural Networks Based Technique for Tea Yield Estimation in Pakistan Using Satellite Imagery. *IEEE Access*, 11, 42578–42594. <https://doi.org/10.1109/ACCESS.2023.3271410>
- [21] Seidlova, A., Kudelcikova, M., Mihalik, J., & Rekus, D. (2021). Interpretation of Remote Sensing Imagery. *IOP Conference Series: Earth and Environmental Science*, 906(1), 012070. <https://doi.org/10.1088/1755-1315/906/1/012070>
- [22] Siahaan, Y., Mataburu, I., & Sucahyanto, S. (2024). Estimasi Produktivitas Lahan Teh Menggunakan Metode NDVI Di Kabupaten Bandung. *Jurnal Ilmiah Wahana Pendidikan*, 10(22), 1337–1347. <https://doi.org/10.5281/zenodo.14599083>
- [23] Skakun, S., Kalecinski, N. I., Brown, M. G. L., Johnson, D. M., Vermote, E. F., Roger, J.-C., & Franch, B. (2021). Assessing within-Field Corn and Soybean Yield Variability from WorldView-3, Planet, Sentinel-2, and Landsat 8 Satellite Imagery. *Remote Sensing*, 13(5), 872. <https://doi.org/10.3390/rs13050872>
- [24] Waspadi, E. A., & Danoedoro, P. (2019). Comparing per-pixel and object-based classification results using two different land-cover/land-use classification schemes: a case study using Landsat-8 OLI imagery. In T. D. Pham, K. D. Kanniah, K. Arai, G. J. P. Perez, Y. Setiawan, L. B. Prasetyo, & Y. Murayama (Eds.), *Sixth International Symposium on LAPAN-IPB Satellite* (p. 126). SPIE. <https://doi.org/10.1117/12.2541876>
- [25] Weiss, M., Jacob, F., & Duveiller, G. (2020). Remote sensing for agricultural applications: A meta-review. *Remote Sensing of Environment*, 236, 111402. <https://doi.org/10.1016/j.rse.2019.111402>
- [26] Yan, K., Gao, Si, Yan, G., Ma, X., Chen, X., Zhu, P., Li, J., Gao, Sicong, Gastellu-Etchegorry, J.-P., Myneni, R. B., & Wang, Q. (2025). A global systematic review of the remote sensing vegetation indices. *International Journal of Applied Earth Observation and Geoinformation*, 139, 104560. <https://doi.org/10.1016/j.jag.2025.104560>